ANTIOXIDANTS & REDOX SIGNALING
Volume 11, Number 10, 2009

DOI: 10.1089/ars.2009.2691

Thioredoxin Binding Protein 2 Modulates Natural Killer T Cell-Dependent Innate Immunity in the Liver: Possible Link to Lipid Metabolism

Hiroaki Okuyama,[1,6] Toru Yoshida,[2,6] Aoi Son,[3] Shin-ichi Oka,[3] Dongmei Wang,[3] Rika Nakayama,[4] Hiroshi Masutani,[3] Hajime Nakamura,[1] Yo-ichi Nabeshima,[5] and Junji Yodoi[3]

Abstract

Thioredoxin binding protein 2 (TBP2) plays a regulatory role in lipid metabolism and immune regulation. We previously reported the effect of TBP2 loss-of-function on lipid metabolism using TBP2 knockout (TBP2KO) mice. In this study, we employed TBP2 transgenic (TBP2TG) mice to analyze the *in vivo* effect of TBP2 gain-of-function. We revealed a decrease in the percentage of hepatic natural killer T (NKT) cells in TBP2KO mice and an increase in the percentage of hepatic NKT cells in TBP2TG mice. The TBP2KO mice were resistant to concanavalin A (ConA)-induced hepatitis, but they were highly susceptible to other types of hepatitis. TBP2 modulates lipid metabolism as well as NKT cell activity. Moreover, TBP2 expression was increased significantly in *klotho*-deficient mice, which exhibit a syndrome resembling aging human phenotypes. TBP2 may play multiple roles in lipid metabolism, innate immunity, and aging. *Antioxid. Redox Signal.* 11, 2585–2593.

Introduction

Thioredoxin (TRX) is a 12-kDa stress-induced protein that exhibits disulfide reduction activity (16). We identified a target molecule of TRX, thioredoxin binding protein 2 (TBP2), by two-hybrid yeast screening (19). TBP2 is identical to the vitamin D_3 upregulated protein 1 (VDUP1) and the thioredoxin interacting protein (Txnip). VDUP1 was originally reported as an upregulated gene in HL-60 cells treated with 1α,25-dihydroxyvitamin D_3, an active form of vitamin D_3 (4). Overexpression of TBP2 in IL-2-independent T cells suppressed the growth (18). TBP2 knockdown caused the IL-2-dependent cells to acquire IL-2-independent partial growth (1). Moreover, we generated TBP2 knockout (TBP2KO) mice to investigate the *in vivo* effect of TBP2 loss-of-function (20). When TBP2KO mice were subjected to fasting conditions, they showed reduced survival rates associated with severe bleeding, dyslipidemia, fatty liver, hypoglycemia, and hepatic and renal dysfunction. In TBP2KO mice, Krebs cycle-mediated fatty acid utilization was impaired, indicating the involvement of TBP2 in the regulation of the lipid metabolism. We suggested that TBP2KO mice might mimic Reye's syndrome, which is a metabolic syndrome due to the disorder of mitochondrial fatty acid β-oxidation, such as acute encephalopathy, hepatic dysfunction, and fatty infiltration of the visceral organs. In this study, we employed TBP2 transgenic (TBP2TG) mice to analyze the *in vivo* effect of TBP2 gain-of-function.

TRX transgenic (TRXTG) mice exhibited extended median and maximum life spans compared with WT mice. Telomerase activity in spleen tissue in TRX-Tg mice was higher than that in WT mice. These results suggest that an overexpression of TRX results in resistance against oxidative stress and a possible extension of life span without apparent abnormality in mammals (14). As TBP2 is an endogenous inhibitor of TRX, we speculate that overexpression of TBP2 may accelerate aging in mice. The contribution of TBP2 to aging is of interest.

Recent studies have suggested an association between lipid metabolism and CD1d-restricted natural killer T (NKT) cells (13). Hepatic NKT cells were depleted in leptin-deficient

[1]Thioredoxin Project, Department of Experimental Therapeutics, Translational Research Center, Kyoto University Hospital, Kyoto, Japan.
[2]Department of Food Sciences and Nutrition, School of Human Environmental Sciences, Mukogawa Women's University, Hyogo, Japan.
[3]Department of Biological Responses, Institute for Virus Research, Kyoto University, Kyoto, Japan.
[4]Laboratory for Animal Resources and Genetic Engineering, Center for Developmental Biology (CDB), RIKEN Kobe, Kobe, Japan.
[5]Department of Pathology and Tumor Biology, Graduate School of Medicine, Kyoto University, Kyoto, Japan.
[6]These authors equally contributed to this work.

ob/ob mice (7). A high fat diet induced fatty liver disease and reduced hepatic NKT cells in mice (12). Fatty hepatocytes from ob/ob mice have significantly less CD1d on their plasma membranes than normal hepatocytes (35). Hepatic NKT cells may play a critical role in the pathogenesis of concanavalin A (ConA)-induced hepatitis, which reflects some aspects of autoimmune hepatitis and viral hepatitis in human patients (29, 30). Therefore, we investigated the role of TBP2 on NKT cell activity during ConA-induced hepatitis using TBP2TG and TBP2KO mice.

Recent studies have shown that VDUP1/TBP2 regulates NK cell activation in the spleen, bone marrow, lymph node, and lung through the regulation of CD122 expression (11). We also found that dendritic cells derived from TBP2KO mice are defective to induce Th1 responses (26). In this study, we investigated the mechanism for the modulation of NKT cell activation by TBP2 using TBP2KO as well as TBP2TG mice.

Materials and Methods

Reagents and antibodies

Concanavalin A (type IV-S) was purchased from Sigma (St. Louis, MO). Fluorescein isothiocyanate (FITC)-conjugated anti-mouse TCR monoclonal antibody (mAb) and phycoerythrin (PE)-conjugated anti-mouse NK1.1 mAb were purchased from BD Pharmingen (San Jose, CA). Purified anti-asialo GM1 (ASGM1) antibody (Ab) was purchased from Wako Pure Chemical Industries, Ltd. (Osaka, Japan).

Animals

The animal protocols employed in this study were approved by the animal research committee at Kyoto University. TBP2KO C57BL/6 background mice were generated in our laboratory, as described previously (20), and bred in our animal laboratory facilities. Human TBP2 cDNA was inserted in the TBP2TG mice between the β-actin promoter and the β-actin terminator (Fig. 1A). Expression of the TBP2 transgene was regulated by a hybrid promoter composed of the cytomegalovirus (CMV) enhancer and chicken β-actin promoter (pCAGGS) (15). The entire cDNA sequence of human TBP2 with EcoRI restriction sites was obtained by the polymerase chain reaction (PCR) from reverse transcripts of human placental total RNA, and cloned into the multiple cloning site (MCS) of pCAGGS. The transgene was microinjected into the pronuclei of fertilized C57B/6 embryos, which were then transplanted into the oviducts of pseudo-pregnant ICR mice as foster mothers. The primers used for RT-PCR were as follows: For mouse TBP2, 5′-ATCCTGGGCTGCAACATCCTCA AAGT-3′ and 5′-CAGGGGCGTACATAAAGATAGGACTG-3′; for human TBP2, 5′-CCGGAATTCCATCATGGTGATG-3′ and 5′-CCGGAATTCCACATGCTCACTGCAC-3′.

In TRXTG mice, the plasmid vector was constructed by inserting human TRX cDNA between the β-actin promoter and the β-actin terminator. To generate TRXTG mice, a 5.5-kb Xba I-Vsp I fragment of the recombinant plasmid was microinjected into the pronuclei of the C57BL/6. Animals were screened by Southern blot analysis of their tail DNA and the presence of TRX transgene was also confirmed by reverse transcription-PCR (14).

Mice that exhibited phenotypes resembling human aging were termed *klotho*-deficient mice and they were obtained by the insertional mutation of the rabbit type I sodium proton exchanger produced by the standard microinjection method. The genetic background of the original *klotho*-deficient mice was a mixture of C57BL/6J and C3H/J (10), and these phenotypes were also confirmed by the reproduction of the null mutation on *klotho* allele itself (32). The animals were housed in an environment with a controlled temperature with light–dark cycles, fed standard mice chow pellets, had access to tap water from the end of each experimental period, and the mice were killed by cervical dislocation under pentobarbital anesthesia.

ConA-induced hepatitis

ConA was dissolved in pyrogen-free PBS and intravenously (i.v.) injected to the mice including TBP2KO, TBP2TG, and control C57BL/6 mice (male, 6 ~ 10 week old) through the tail vein at a dose of 15 mg/kg body weight. Control mice received an i.v. injection of PBS.

Histology

For the histopathological studies, harvested livers were fixed in 10% buffered formalin and embedded in paraffin. Five-micrometer sections were affixed to slides, deparaffinized, and stained with hematoxylin–eosin to assess morphologic changes.

Preparation of liver mononuclear cells

Liver mononuclear cells were isolated as described previously with minor modifications (33). Briefly, the liver mononuclear cells were separated by density gradient centrifugation. The liver mononuclear cells were studied for the expression of cell surface markers and used for cell sorting and adoptive transfer.

Flow cytometry

The surface phenotype of the cells was characterized by two-color flow cytometry. After preincubation with anti-mouse CD16/32 (2.4G2) mAb, the cells were incubated with a saturating amount of FITC-conjugated anti-mouse TCR mAb and PE-conjugated anti-mouse NK1.1 (PK136) mAb, and analyzed on a FACS caliber (Becton Dickinson, San Jose, CA). Data acquisition was performed with FlowJo (TreeStar Inc. Ashland, OR).

RT and quantitative PCR

Total RNA extraction and cDNA synthesis was performed as previously described (21). Real time PCR was performed using the iQ SYBR Green Supermix and iCycler Real Time PCR Detection System (Bio-Rad Laboratories, Hercules, CA). For each set of primers, gradient PCR was performed for determination of optimal annealing temperature. The sequences of the PCR primers were as follows: Mouse IL-2 5′-GTGCTC CTTGTCAACAGCG-3′ and 5′-GGGGAGTTTCAGGTTCC TGTA-3′; mouse IL-15 5′-GAGGAATACATCCATCTCGTGC-3′ and 5′-CCTACACTGACACAGCCCAAAA-3′; mouse MTP 5′-GTGGAGGAATCCTGATGGTGA-3′ and 5′-TGATCTTA GGTGTACTTTTGCCC-3′; mouse Fyn 5′-ATGGGCTGTGTG CAATGTAAGG-3′ and 5′-CCAATCCAGAAGTTTGTGG GG-3′; mouse RelB 5′-GATCATGACAGCTACGGTG-3′ and 5′-GGCAAAGCCATCGTCCAG-3′; mouse SAP 5′-CCTGTAA

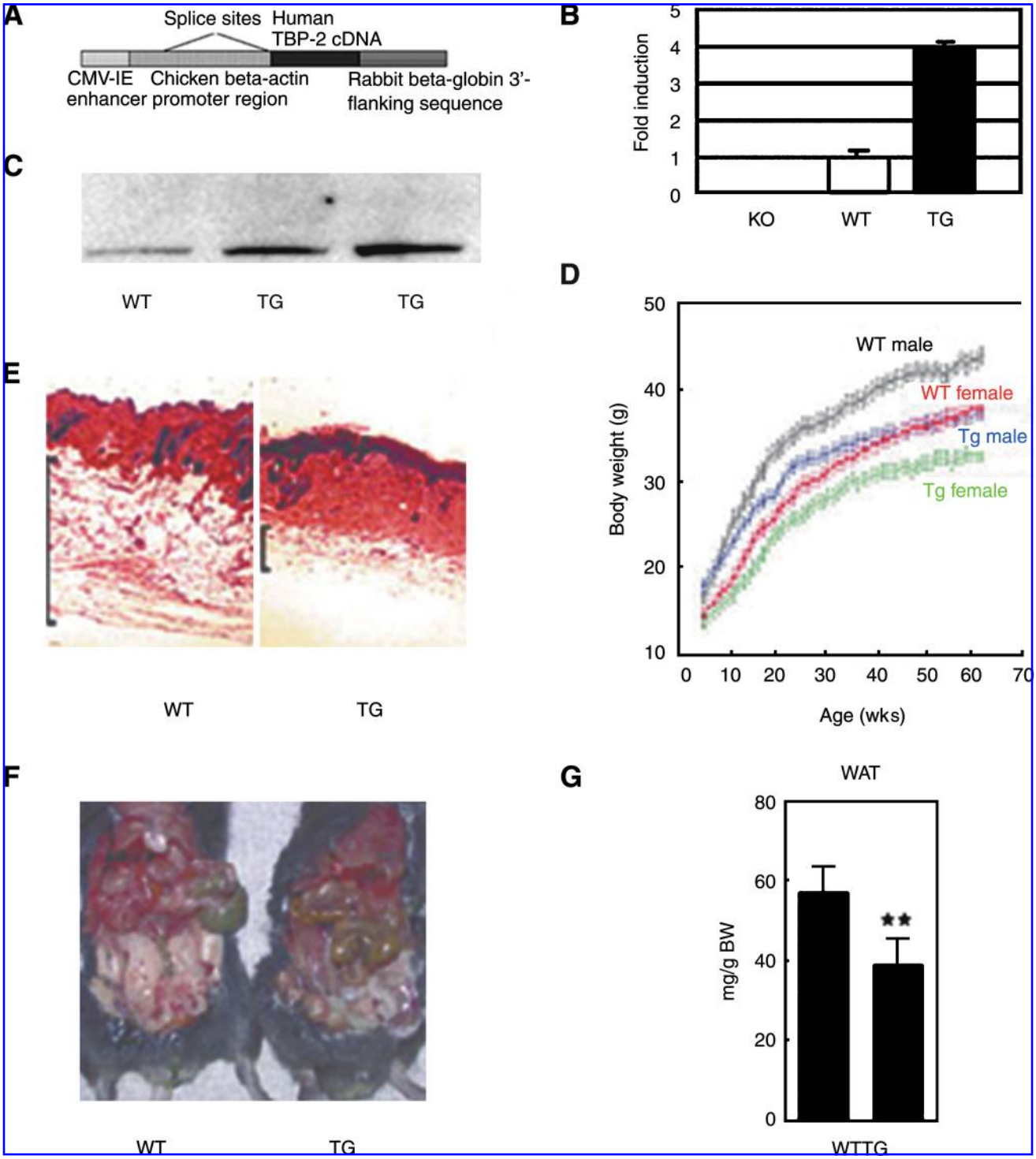

FIG. 1. Generation of TBP2TG mice. (**A**) Constructed transgene of human TBP2. (**B**) TBP2 mRNA expression in the liver by real time PCR. (**C**) Expression of TBP-2 protein in the liver of wild-type and TBP2TG mice by Western blot analysis. (**D**) Growth curves of male and female mice up to 60 wk. *Black open boxes*: WT males ($n = 6$), *blue filled circles*: TBP2TG males ($n = 8$), *red filled boxes*: WT females ($n = 6$), and *green open circles*: TBP2TG females ($n = 8$). (**E**) HE staining of a tissue section of subcutaneous fat of the old male mice (~90 weeks old). Typical images of subcutaneous fat in the abdomen are indicated by thick lines. (**F**) White adipose tissue of male (~45 weeks old) mice. The images shown are typical examples taken around the internal organs. (**G**) Weight of white adipose tissue in the abdomen. (For interpretation of the references to color in this figure legend, the reader is referred to the web version of this article at www.liebertonline.com/ars).

TAGCATCTCGCCTGAT-3′ and 5′-AGTTTTCCAATCCGC ACTTTAAAG -3′.

Real time PCR was performed using iQ SYBR Green Supermix and iCycler Real time PCR Detection System (Bio-Rad Laboratories). For each set of primers, gradient PCR was performed for determination of optimal annealing temperature. Serial dilutions of cDNA samples were analyzed to determine efficiency and the dynamic range of the PCR. Stringent assay requirements were imposed as follows: (a) standard deviation for the cycle threshold (CT) among three to five replicate samples <0.3; (b) correlation coefficient of plot of CT *versus* log (ng input RNA) >0.99; (c) difference of <5% in PCR efficiency (E) of samples to be compared, calculated using the formula $E = (10^{-1/m}) - 1$, where m is the slope of the best fit line for CT *versus* log (ng input RNA). The expression of each target mRNA relative to 18 S rRNA (R) under an experimental, as compared with control, condition was calculated based on the threshold cycle (CT) as $r = 2^{-\Delta(\Delta CT)}$, where $\Delta C_T = C_{T\ \text{target}} - C_{T\ 18S}$ and $\Delta(\Delta CT) = \Delta C_{T\ \text{experimental}} - \Delta C_{T\ \text{control}}$.

Western blot analysis

Liver samples were lysed with RIPA buffer, and the extracts were cleaned by centrifugation. Equal amounts of protein (100 μg), as estimated by the Bradford method using a protein assay (Bio-Rad Laboratories Inc.), were electrophoresed on a 10% SDS-polyacrylamide gel, and proteins were then electrophoretically transferred to a poly membrane (Millipore Corp., Billerica, MA), according to the manufacturer's instructions.

NKT cell depletion

To deplete NK and/or NKT cells, the mice were treated i.p. with 500 μg of either control Ab or anti-NK1.1 (PK136) mAb and/or anti-asialo GM1 (ASGM1) Ab on day 0 and day 3 (2, 24, 31). On day 4, each group was injected with 15 mg/kg of Con A, and mouse sera were collected 18 h later.

Isolation of primary-cultured hepatocyte and Ito cell from the mice

Primary hepatocytes and hepatic stellate cells (HSC) were obtained from murine livers as previously described (22). Cell purity was always more than 95% as assessed by a typical star-like configuration and by detecting vitamin A autofluorescence.

Insulin reduction assay

The activity of TRX was determined by the insulin reduction assay, according to the method described previously with minor modifications (9, 19). After homogenizing tissue, the supernatants were added to a DTT activation buffer (1 *M* Tris-HCl (pH 7.5), 100 m*M* EDTA-Na (pH 7.5), 20 mg/ml bovine serum albumin (BSA), and 100 m*M* DTT) at 37°C for 30 min, and then incubated with the reaction mixture of 1 *M* Tris-HCl (pH 7.5), 100 m*M* EDTA-Na (pH 7.5), 2 m*M* NADPH (Wako Pure Chemical Industries, Ltd., Osaka, Japan), and 1 U/ml yeast TRX reductase (Oriental Yeast Co. Ltd., Tokyo, Japan) at 25°C. The reduction in absorbance at 340 nm was measured with a spectrophotometer at 15 s intervals. The values of /Vmax/ (ΔOD/min) were determined from Lineweaver–Burk plots (Softmax software, Molecular Devices, CA).

Statistics

The values presented as bar graphs are means ± standard deviation (SD). The differences between groups were examined for significance with Student's t-test, with p values <0.05 considered significant.

Results

Generation of TBP2TG mice

We generated TBP2TG mice lines. Fusion of the entire human TBP2 coding sequence with the chicken beta-actin promoter region and the rabbit β-globin 3′ non-coding sequence (Fig. 1A) was confirmed by Southern blotting (data not shown) and RT-PCR using TBP2 primer (Fig. 1B). To estimate the overall expression of TBP2, we performed Western blotting using an antibody recognizing both mouse and human TBP2, and showed an approximately threefold increase in the expression of TBP2 in the liver of TBP2TG mice (Fig. 1C).

The body weight of the TBP2TG mice was consistently 10%–15% lower after weaning, compared with age-matched and sex-matched WT mice (Fig. 1D). The volume of subcutaneous fat seemed to be lower in TBP2TG mice, compared with the WT mice (Fig. 1E). The weight of white adipose tissue and subcutaneous fat was significantly lower in TBP2TG mice (Fig. 1F), and the actual weight of white adipose tissue was decreased in TBP2TG mice (Fig. 1G).

TBP2 modulates the percentage of NKT cell in the liver

In the liver, TBP2KO mice had a significantly less number of hepatic NKT cells than that shown in WT mice, whereas TBP2TG mice had a significantly higher number of hepatic NKT cells (Fig. 2). No significant changes were observed in hepatic NK cells between the KO, WT, and TG animals (Fig. 2). Hepatic NKT cells are known to play a critical role in the pathogenesis of ConA-induced hepatitis (29). In order to investigate the *in vivo* effect of TBP2 on NKT cell function, we subjected genetic engineered mice to ConA-induced hepatitis. Histological findings showed the area of necrotic change was smaller in the liver of TBP2KO mice than in WT mice, whereas the area of necrotic change was wider in the liver of TBP2TG mice than in WT mice (Fig. 3A). Consistent with the histological findings, the serum ALT level was significantly reduced in TBP2KO mice, compared with WT mice after ConA administration, whereas the serum ALT level was significantly increased in TBP2TG mice (Fig. 3B).

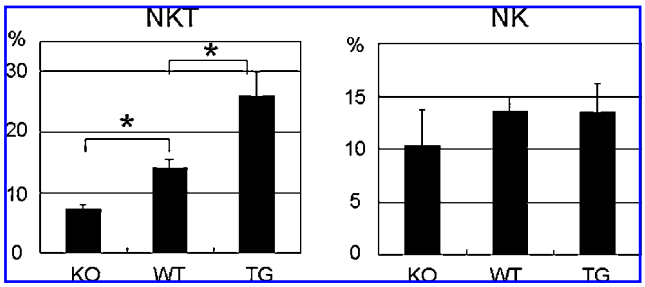

FIG. 2. NKT cell population in TBP2KO and TBP2TG mice. The percentage of NKT and NK cells in the liver mononuclear cells. Results are expressed as the mean ± SD of three mice per group. *$p < 0.05$.

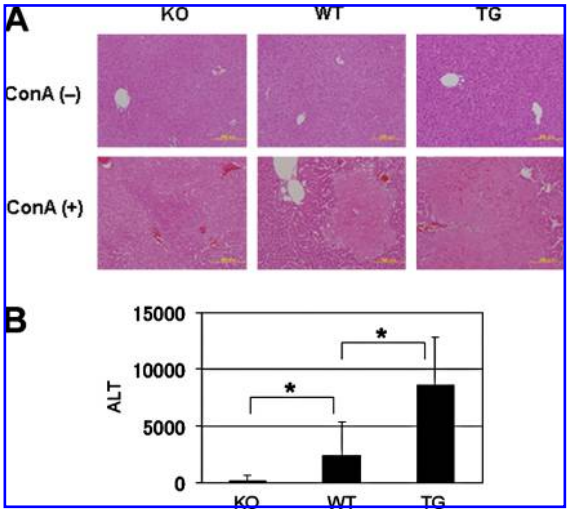

FIG. 3. ConA-induced hepatitis in TBP2KO and TBP2TG mice. (**A**) Histology in the liver. HE staining of the livers 18 h after ConA injection. Data are representative of nine independent experiments in each group. (**B**) ALT levels in the serum. Mice were injected i.v. with ConA (15 mg/kg). After 18 h, serum ALT levels were measured. Data were collected from nine mice in each group. Results are expressed as the mean ± SD of nine mice per group. $*p < 0.05$. (For interpretation of the references to color in this figure legend, the reader is referred to the web version of this article at www.liebertonline.com/ars).

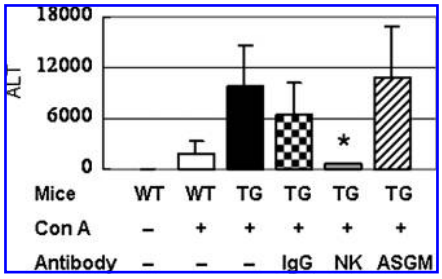

FIG. 4. Hepatic NKT cells are critical for ConA-induced hepatitis in TBP2TG mice. Blocking NKT cell function by antibody. TBP2TG mice were injected i.p. with antibody against NK1.1 (500 μg) or asialo GM1 (500 μg) on day 0 and 3. On day 4, TBP2Tg mice were injected with ConA. Eighteen hours after ConA injection, the serum ALT levels were measured. *Lane 1*: WT mice control, *lane 2*: WT mice injected with ConA (*white bar*), *lane 3*: TBP2TG mice injected with ConA (*black bar*), *lane 4:* TBP2TG mice pretreated with control IgG (*dotted bar*), *lane 5*: TBP2TG mice pretreated with anti-NK1.1 antibody (*gray bar*), *lane 6*: TBP2TG mice pretreated with anti-asialo GM1 antibody (*hatched bar*). Data are collected from three independent experiments. Results are expressed as the mean ± SD of three mice per group. $*p < 0.05$.

Hepatic NKT cells are critical for ConA-induced hepatitis in TBP2TG mice

We conducted tests to determine if hepatic NKT cells caused severe hepatitis in TBP2TG mice. Treatment with anti-NK1.1 monoclonal antibody (mAb), which depletes NK and NKT cells *in vivo*, inhibited ConA-induced hepatitis in TBP2TG mice (Fig. 4). However, treatment with anti-asialo GM1 Ab, which depletes NK but not NKT cells, did not affect the instances of ConA-induced hepatitis in TBP2TG mice (Fig. 4). These results indicate that hepatic NKT cells, not NK cells, contribute to ConA-induced hepatitis, and hepatic NKT cells cause severe hepatitis in TBP2TG mice.

Altered gene expression in the liver by TBP2

In order to investigate how TBP2 regulates the percentage of hepatic NKT cell, we analyzed the mRNA expression of various genes related to NKT cell activation and development, and conducted RT-PCR (Fig. 5A). The gene expression of IL-2 in TBP2KO mice was less than that shown in WT mice, whereas IL-2 in TBP2TG mice was more than that shown in WT mice. IL-15 expression in TBP2KO mice was less than that shown in WT mice. However, IL-15 expression in TBP2TG mice was not more than that shown in WT mice. The gene expression of microsomal triglyceride transfer protein (MTP), which is loading CD1d with lipids in the endoplasmic reticulum and endosomal compartments, were less in TBP2KO mice than that shown in WT mice (3). However, MTP in TBP2TG mice was not more than that shown in WT mice.

The signaling lymphocytic activation molecule (SLAM)-associated protein, SAP, and the Src family tyrosine kinase, Fyn, play a crucial role during NKT development (6, 17). RelB, one of the Rel/NF-κB proteins, also plays an essential role during NKT cell development (25). There was no difference in Fyn expression among the TBP2KO, WT, and TBP2TG mice. RelB and SAP expression in TBP2KO mice was almost same as that in the WT mice, although the gene expression of these molecules in TBP2TG mice was more than that shown in WT mice. These results indicate that only IL-2 was related to TBP2 expression in the liver, and IL-2 might contribute to the effect of TBP2 on the number of hepatic NKT cells.

CD1d and CD122 expression

CD1d is a family of major histocompatibility complex (MHC) class I-related molecules that functions in glycolipid and lipid antigen presentation to NKT cells (8). A recent study showed that fatty hepatocytes from ob/ob mice have significantly less CD1d on their plasma membranes than normal hepatocytes. However, we did not find any correlation between TBP2 and CD1d expression in CD11c dendritic cells, F4/80 macrophages, hepatocytes and Ito cells (Figs. 5B and 5C). Another recent study showed VDUP1/TBP2 regulates NK cell activation in the spleen, bone marrow, lymph node, and lung through the regulation of CD122 expression. However, we did not find any correlation between TBP2 and CD122 expression in hepatic NKT cells (Fig. 5D).

TRX is known to be a negative regulator of TBP2 (19). To check whether TRX contributes to TBP2-dependent regulation of hepatic NKT cell activation, we analyzed the percentage of hepatic NKT cells in TRX transgenic (TRXTG) mice. The percentage of hepatic NKT cells in the liver of TRXTG mice was almost the same as that shown in WT mice (Fig. 5E).

Moreover, we checked the possible roles of TBP2 in the regulation of aging, because some of the phenotypes in TBP2TG mice were similar to the phenotypes in the *klotho*-deficient mice (10). The expression of the TBP2 gene was three times higher in the *klotho*-deficient mice than that shown in the WT mice, even without the administration of 1α,25-dihydroxyvitamin D_3 (Fig. 5F). TBP2 expression was

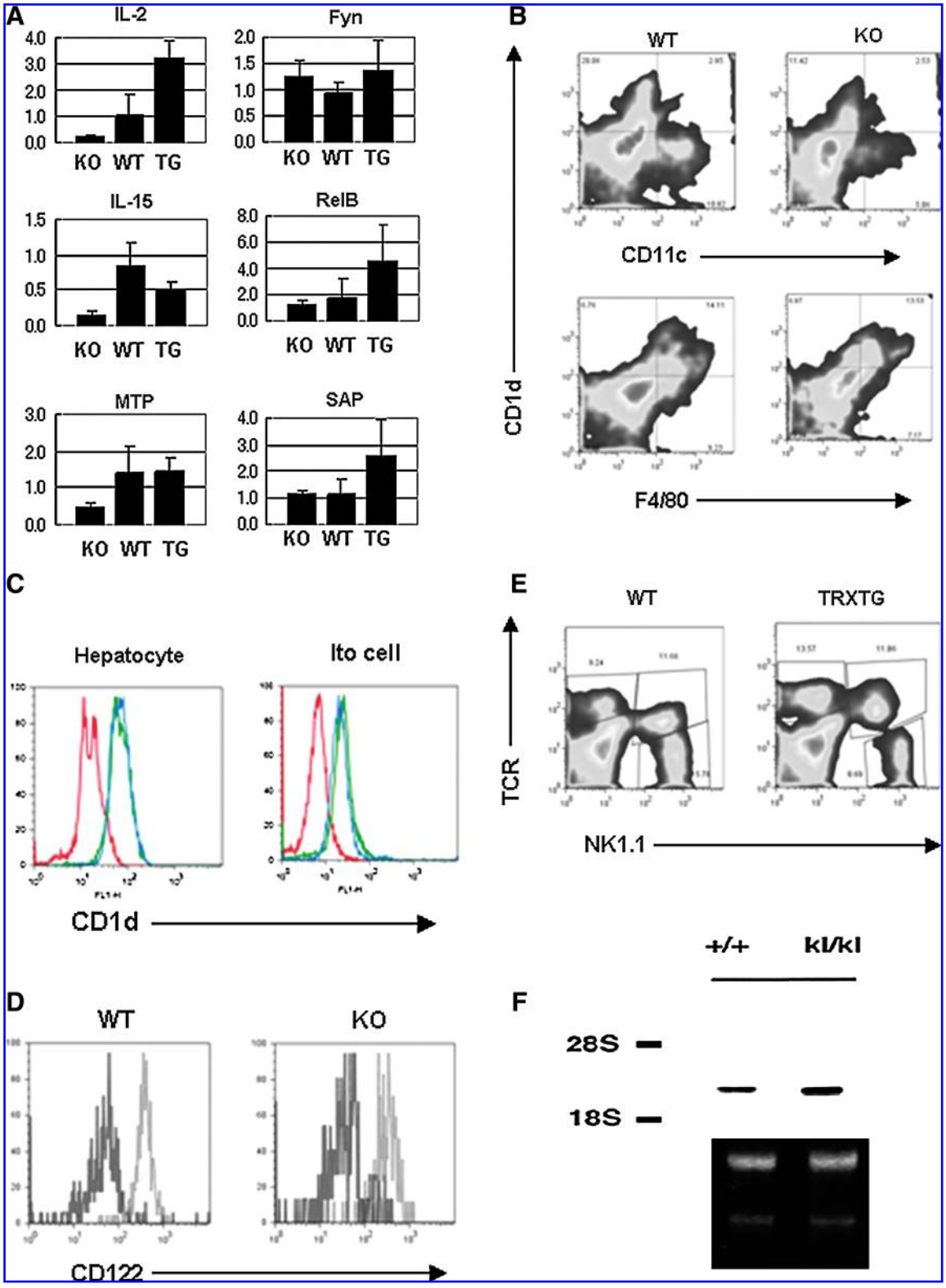

FIG. 5. CD1d and CD122 expression. (**A**) Analysis of gene expression in the liver by real time PCR. (**B**) CD1d expression in $CD11c^+$ dendritic cell and $F4/80^+$ macrophage. (**C**) CD1d expression in hepatocyte and Ito cell. *Green line*: WT mice, *blue line*: TBP2KO mice, *red line*: isotype control. (**D**) CD122 expression in hepatic NKT cell. *Gray line*: CD122 expression, *black line*: isotype control. (**E**) NKT cell population in the liver of TRXTG mice. (**F**) TBP2 gene expression in *klotho*-deficient mice analyzed by Northern blot. (For interpretation of the references to color in this figure legend, the reader is referred to the web version of this article at www.liebertonline.com/ars).

increased significantly in *klotho*-deficient mice, which exhibit a syndrome resembling human aging phenotypes.

Discussion

In this study, we generated TBP2TG mice to investigate the *in vivo* effect of TBP2 gain-of-function. TBP2TG mice showed a high level of glucose in the serum under fasting conditions, and a low level of pyruvate and lactate in the plasma, strongly suggesting upregulations of the TCA cycle (data not shown). As expected, all of the results found in TBP2TG mice were opposite to those found in TBP2KO mice, in terms of lipid and glucose metabolism (20). These results clearly indicate that TBP2 profoundly contributes to lipid and glucose metabolism. TBP2TG mice exhibited growth retardation after weaning, associated with the reduction of the amount of subcutaneous fat (Figs. 1D–1G). We also observed a lower reducing activity of the endogenous TRX and enhanced production of ROS in TBP2TG mice (data not shown), suggesting that oxidative stress was increased in TBP2TG mice.

It is noteworthy that these phenotypes in TBP2TG mice were partially similar to the *klotho*-deficient mice (10). Some phenotypes of the *klotho*-deficient mice can be explained by excessive vitamin D levels leading to altered calcium and phosphorus metabolism (32, 36), but an elucidation for the massive reduction of white adipose tissues and other lipid markers associated with aging has remained unknown. In this study, we found that the expression of TBP2 increased drastically in the *klotho*-deficient mice (Fig. 5F). We speculated that TBP2 overexpression may partially contribute to the phenotype resembling aging. The possible roles of TBP2 in the regulation of aging have also been discussed (37, 38).

In this study, we found that the percentage of hepatic NKT cells in TBP2TG mice was twice that in the WT mice, and the percentage of hepatic NKT cells in TBP2KO mice was half that in the WT mice. Lee *et al*. reported that TBP2KO mice showed a profound reduction of NK cells in the spleen, bone marrow, lymph node, and lung through the regulation of CD122 expression (11). We speculated that there is a liver-specific mechanism related to how TBP2 regulates the number of hepatic NKT cells rather than NK cells in the liver.

NKT cells are selected exclusively by CD1d-glycolipid complexes expressed by other cortical $CD4^+CD8^+$ thymocytes (28). However, we did not find any difference in CD1d expression (Figs. 5B–5D). Recently, it has been reported that the signaling lymphocytic activation molecule (SLAM)-associated protein SAP plays a crucial role during NKT development (17, 23). Fyn, RelB, IκB, and NF-κB also contribute to NKT cell development (5, 6, 25, 27, 34). However, we did not find any difference in the expression of these genes (Fig. 5A). IL-2 expression in TBP2KO mice was less than that shown in the WT mice, whereas IL-2 in TBP2TG mice was more than that shown in the WT mice (Fig. 5A), indicating IL-2 might contribute to the effect of TBP2 on NKT cell population.

The blockade of lipid catabolism in TBP2KO mice may result in the deficiency of endogenous ligands (lipid antigens) for NKT cell activation, whereas the enhancement of lipid mobilization in TBP2TG mice may increase lipid antigens on CD1d to promote NKT cell activation, resulting in prominent inflammatory and immune response. Acute hepato-renal failure in the TBP2KO mice under fasting conditions could be due to energy deficiency. Indeed, glucose could rescue acute hepato-renal failure in the TBP2KO mice under fasting conditions, as is the case with Reye's syndrome. The marked deviation of NKT cell population in TBP2KO and TBP2TG mice indicates that endogenous ligands for NKT activation might be under the control of TBP2-dependent lipid oxidation.

ConA-induced hepatitis in mice represents viral hepatitis and autoimmune hepatitis in human. TBP2 regulates not only hepatic inflammation through NKT cells but also lipid metabolism, suggesting that TBP2 plays a role in the pathogenesis of human liver diseases. Recently, we found that methionine-choline deficient (MCD) diet-induced inflammation was attenuated in TBP2KO mice (Ahsan *et al*., in press), suggesting that TBP2 may also be involved in the development of nonalcoholic steatohepatitis (NASH) in humans. The modulation of TBP2 could offer a novel approach in the treatment of human liver diseases in the future.

In conclusion, our findings provide evidence that TBP2 regulates lipid metabolism and hepatic NKT cell activity to control ConA-induced hepatitis.

Acknowledgments

We would like to express our thanks to Ms. Akie Teratani (Redox Bioscience Inc. Kyoto, Japan), Suzuyo Furukawa (Thioredoxin Project, Kyoto University Hospital), and Mr. Akira Yamada (Redox Bioscience Inc. Kyoto, Japan) for their technical support, Ms. Kyoko Miyamoto (Thioredoxin Project, Kyoto University Hospital) for her secretarial support, and Dr. Yuma Hoshino (Thioredoxin Project, Kyoto University Hospital), Dr. Ahsan Kaimul (Thioredoxin Project, Kyoto University Hospital), Dr. Akira Mitsui (Ajinomoto Inc, Japan), Dr. Yoshiyuki Matsuo (Institute for Virus Research, Kyoto University) for their critical discussion. This work was supported by a Grant-in-Aid for the Creation of Innovations through Business-Academic-Public Sector Cooperation and Open Competition for the Development of Innovative Technology, from the Ministry of Education, Culture, Sports, Science, and Technology of Japan. This work was also supported in part by the Program for the Promotion of Fundamental Studies in Health Sciences of the National Institute of Biomedical Innovation (NIBIO).

Author Disclosure Statement

No competing financial interests exist.

References

1. Ahsan MK, Masutani H, Yamaguchi Y, Kim YC, Nosaka K, Matsuoka M, Nishinaka Y, Maeda M, and Yodoi J. Loss of interleukin-2-dependency in HTLV-I-infected T cells on gene silencing of thioredoxin-binding protein-2. *Oncogene* 25: 2181–2191, 2006.
2. Anand S, Wang P, Yoshimura K, Choi IH, Hilliard A, Chen YH, Wang CR, Schulick R, Flies AS, Flies DB, Zhu G, Xu Y, Pardoll DM, Chen L, and Tamada K. Essential role of TNF family molecule LIGHT as a cytokine in the pathogenesis of hepatitis. *J Clin Invest* 116: 1045–1051, 2006.
3. Brozovic S, Nagaishi T, Yoshida M, Betz S, Salas A, Chen D, Kaser A, Glickman J, Kuo T, Little A, Morrison J, Corazza N, Kim JY, Colgan SP, Young SG, Exley M, and Blumberg RS.

CD1d function is regulated by microsomal triglyceride transfer protein. *Nat Med* 10: 535–539, 2004.
4. Chen KS and DeLuca HF. Isolation and characterization of a novel cDNA from HL-60 cells treated with 1, 25-dihydroxyvitamin D-3. *Biochem Biophys Acta* 1219: 26–32, 1994.
5. Czar MJ, Kersh EN, Mijares LA, Lanier G, Lewis J, Yap G, Chen A, Sher A, Duckett CS, Ahmed R, and Schwartzberg PL. Altered lymphocyte responses and cytokine production in mice deficient in the X-linked lymphoproliferative disease gene SH2D1A/DSHP/SAP. *Proc Natl Acad Sci USA* 98: 7449–7454, 2001.
6. Eberl G, Lowin–Kropf B, and MacDonald HR. Cutting edge: NKT cell development is selectively impaired in Fyn-deficient mice. *J Immunol* 163: 4091–4094, 1999.
7. Guebre–Xabier M, Yang S, Lin HZ, Scwenk R, Krzych U, and Diehl AM. Altered hepatic lymphocyte subpopulations in obesity-related murine fatty livers: Potential mechanism for sensitization to liver damage. *Hepatology* 31: 633–640, 2000.
8. Gumperz JE, Roy C, Makowska A, Lum D, Sugita M, Podrebarac T, Koezuka Y, Porcelli SA, Cardell S, Brenner MB, and Behar SM. Murine CD1d-restricted T cell recognition of cellular lipids. *Immunity* 12: 211–221, 2000.
9. Holmgren A and Bjornstedt M. Thioredoxin and thioredoxin reductase. *Method Enzymol* 252: 199–208, 1995.
10. Kuro–o M, Matsumura Y, Aizawa H, Kawaguchi H, Utsugi T, Ohyama Y, Kurabayashi M, Kaname T, Kume E, Iwasaki H, Iida A, Shiraki–Iida T, Nishikawa S, Nagai R, and Nabeshima YI. Mutation of the mouse klotho gene leads to a syndrome resembling ageing. *Nature* 390: 45–51, 1997.
11. Lee KN, Kang HS, Jeon JH, Kim EM, Yoon SR, Song H, Lyu CY, Piao ZH, Kim SU, Han YH, Song SS, Lee YH, Song KS, Kim YM, Yu DY, and Choi I. VDUP1 is required for the development of natural killer cells. *Immunity* 22: 195–208, 2005.
12. Li Z, Soloski MJ, and Diehl AM. Dietary factors alter hepatic innate immune system in mice with nonalcoholic fatty liver disease. *Hepatology* 42: 880–885, 2005.
13. Major AS, Joyce S, and Kaer LV. Lipid metabolism, atherogenesis and CD1-restricted antigen presentation. *Trends Mol Med* 12: 270–278, 2006.
14. Mitsui A, Hamuro J, Nakamura H, Kondo N, Hirabayashi Y, Ishizaki–Koizumi S, Hirakawa T, Inoue T, and Yodoi J. Overexpression of human thioredoxin in transgenic mice controls oxidative stress and life span. *Antioxid Redox Signal* 4: 693–696, 2002.
15. Miyazaki J, Takaki S, Araki K, Tashiro F, Tominaga A, Takatsu K, and Yamamura K. Expression vector system based on the chicken beta-actin promoter directs efficient production of interleukin-5. *Gene* 79: 269–277, 1989.
16. Nakamura H, Nakamura K, and Yodoi J. Redox regulation of cellular activation. *Annu Rev Immunol* 15: 351–369, 1997.
17. Nichols KE, Hom J, Gong SY, Ganguly A, Ma CS, Cannons JL, Tangye SG, Schwartzberg PL, Koretzky GA, and Stein PL. Regulation of NKT cell development by SAP, the protein defective in XLP. *Nat Med* 11: 340–345, 2005.
18. Nishinaka Y, Nishiyama A, Masutani H, Oka S, Ahsan KM, Nakayama Y, Ishii Y, Nakamura H, Maeda M, and Yodoi J. Loss of thioredoxin-binding protein-2/vitamin D3 up-regulated protein 1 in human T-cell leukemia virus type I-dependent T-cell transformation: Implications for adult T-cell leukemia leukemogenesis. *Cancer Res* 64: 1287–1292, 2004.
19. Nishiyama A, Matsui M, Iwata S, Hirota K, Masutani H, Nakamura H, Takagi Y, Sono H, Gon Y, and Yodoi J. Identification of thioredoxin-binding protein-2/vitamin D_3 up-regulated protein 1 as a negative regulator of thioredoxin function and expression. *J Biol Chem* 274: 21645–21650, 1999.
20. Oka S, Liu W, Masutani H, Hirata H, Shinkai Y, Yamada S, Yoshida T, Nakamura H, and Yodoi J. Impaired fatty acid utilization in thioredoxin binding protein-2 (TBP-2)-deficient mice: A unique animal model of Reye syndrome. *FASEB J* 20: 121–123, 2006.
21. Okuyama H, Krishnamachary B, Zhou YF, Nagasawa H, Bosch–Marce M, and Semenza GL. Expression of vascular endothelial growth factor receptor 1 in bone marrow-derived mesenchymal cells is dependent on hypoxia-inducible factor 1. *J Biol Chem* 281: 15554–15563, 2006.
22. Okuyama H, Nakamura H, Shimahara Y, Uyama N, Kwon YW, Kawada N, Yamaoka Y, and Yodoi J. Overexpression of thioredoxin prevents thioacetamide-induced hepatic fibrosis in mice. *J Hepatol* 42: 117–123, 2005.
23. Sayos J, Wu C, Morra M, Wang N, Zhang X, Allen D, van Schaik S, Notarangelo L, Geha R, Roncarolo MG, Oettgen H, De Vries JE, Aversa G, and Terhorst C. The X-linked lymphoproliferative-disease gene product SAP regulates signals induced through the co-receptor SLAM. *Nature* 395: 462–469, 1998.
24. Seaman WE, Sleisenger M, Eriksson E, and Koo GC. Depletion of natural killer cells in mice by monoclonal antibody to NK-1.1. Reduction in host defense against malignancy without loss of cellular or humoral immunity. *J Immunol* 138: 4539–4544, 1987.
25. Sivakumar V, Hammond KJL, Howells N, Pfeffer K, and Weih F. Differential requirement for Rel/nuclear factor kappa B family members in natural killer T cell development. *J Exp Med* 197: 1613–1621, 2003.
26. Son A, Nakamura H, Okuyama H, Oka S, Yoshihara E, Liu W, Matsuo Y, Kondo N, Masutani H, Ishii Y, Iyoda T, Inaba K, and Yodoi J. Dendritic cells derived from TBP-2-deficient mice are defective in inducing T cell responses. *Eur J Immunol* 38: 1358–1367, 2008.
27. Stanic AK, Bezbradica JS, Park JJ, Van Kaer L, Boothby MR, and Joyce S. Cutting edge: the ontogeny and function of Va14Ja18 natural T lymphocytes require signal processing by protein kinase C theta and NF-kappa B. *J Immunol* 172: 4667–4671, 2004.
28. Sugita M, Cernadas M, and Brenner M. New insights into pathways for CD1-mediated antigen presentation. *Curr Opin Immunol* 16: 90–95, 2004.
29. Takeda K, Hayakawa Y, Van Kaer L, Matsuda H, Yagita H, and Okumura K. Critical contribution of liver natural killer T cells to a murine model of hepatitis. *Proc Natl Acad Sci USA* 97: 5498–5503, 2000.
30. Tiegs G, Hentschel J, and Wendel A. A T cell-dependent experimental liver injury in mice inducible by concanavalin A. *J Clin Invest* 90: 196–203, 1992.
31. Toyabe S, Seki S, Iiai T, Takeda K, Shirai K, Watanabe H, Hiraide H, Uchiyama M, and Abo T. Requirement of IL-4 and liver NK1+ T cells for concanavalin A-induced hepatic injury in mice. *J Immunol* 159: 1537–1542, 1997.
32. Tsujikawa H, Kurotani Y, Fujimori T, and Nabeshima Y. Klotho, a gene related to a syndrome resembling human premature aging, functions in a negative regulatory circuit of vitamin D endocrine system. *Mol Endocrinol* 17: 2393–2403, 2003.
33. Watanabe H, Ohtsuka K, Kimura M, Ikarashi Y, Ohmori K, Kusumi A, Ohteki T, Seki S, and Abo T. Details of an isolation method for hepatic lymphocytes in mice. *J Immunol Meth* 146: 145–154, 1992.
34. Wu C, Nguyen KB, Pien GC, Wang N, Gullo C, Howie D, Sosa MR, Edwards MJ, Borrow P, Satoskar AR, Sharpe AH,

Biron CA, and Terhorst C. SAP controls T cell responses to virus and terminal differentiation of TH2 cells. *Nat Immunol* 2: 410–414, 2001.
35. Yang L, Jhaveri R, Huang J, Qi Y, and Diehl AM. Endoplasmic reticulum stress, hepatocyte CD1d and NKT cell abnormalities in murine fatty livers. *Lab Invest* 87: 927–937, 2007.
36. Yoshida T, Fujimori T, and Nabeshima Y. Mediation of unusually high concentrations of 1, 25-dihydroxyvitamin D in homozygous klotho mutant mice by increased expression of renal 1 α-hydroxylase gene. *Endocrinology* 143: 683–689, 2002.
37. Yoshida T, Nakamura H, Masutani H, and Yodoi J. The involvement of thioredoxin and thioredoxin binding protein-2 on cellular proliferation and aging process. Ann NY Acad Sci 1055: 1–12, 2003.
38. Yoshida T, Oka S, Masutani H, Nakamura H, and Yodoi J. The role of thioredoxin in the aging process: Involvement of oxidative stress. *Antioxid Redox Signal* 5: 563–570, 2003.

Address correspondence to:
Junji Yodoi
Department of Biological Responses
Institute for Virus Research
Kyoto University
53 Shogoin
Kawaharacho, Sakyo-ku
Kyoto 606-8507, Japan

E-mail: yodoi@virus.kyoto-u.ac.jp

Date of first submission to ARS Central, June 2, 2009; date of final revised submission, July 16, 2009; date of acceptance, July 20, 2009.

Abbreviations Used

CMV = cytomegalovirus
ConA = concanavalin A
DMEM = Dulbecco's Modified Eagle Medium
FBS = fetal bovine serum
FITC = fluorescein isothiocyanate
HBSS = Hanks' balanced salt solution
i.v. = intravenously
mAb = monoclonal antibody
MCD = methionine-choline deficient
MCS = multiple cloning site
MHC = major histocompatibility complex
MTP = microsomal triglyceride transfer protein
NASH = nonalcoholic steatohepatitis
NK = natural killer
NKT = natural killer T
PBS = phosphate-buffered saline
pCAGGS = chicken β-actin promoter
PCR = polymerase chain reaction
PE = phycoerythrin
ROS = reactive oxygen species
SAP = SLAM-associated protein
SLAM = signaling lymphocytic activation molecule
TBP2 = thioredoxin binding protein 2
TBP2KO = TBP2 knockout
TBP2TG = TBP2 transgenic
TRX = hioredoxin
TRXTG = TRX transgenic
Txnip = thioredoxin interacting protein
VDUP1 = vitamin D_3 up-regulated protein 1

This article has been cited by:

1. Samuel Lee , Soo Min Kim , Richard T. Lee . Thioredoxin and Thioredoxin Target Proteins: From Molecular Mechanisms to Functional Significance. *Antioxidants & Redox Signaling*, ahead of print. [Abstract] [Full Text HTML] [Full Text PDF] [Full Text PDF with Links]
2. Oded N. Spindel , Cameron World , Bradford C. Berk . 2012. Thioredoxin Interacting Protein: Redox Dependent and Independent Regulatory Mechanisms. *Antioxidants & Redox Signaling* **16**:6, 587-596. [Abstract] [Full Text HTML] [Full Text PDF] [Full Text PDF with Links]
3. Shin-ichi Oka, Wenrui Liu, Eiji Yoshihara, Md. Kaimul Ahsan, Dorys Adriana Lopez Ramos, Aoi Son, Hiroaki Okuyama, Li Zhang, Hiroshi Masutani, Hajime Nakamura, Junji Yodoi. 2010. Thioredoxin binding protein-2 mediates metabolic adaptation in response to lipopolysaccharide in vivo. *Critical Care Medicine* **38**:12, 2345-2351. [CrossRef]
4. Md. Kaimul Ahsan , Hiroaki Okuyama , Yuma Hoshino , Shin-Ichi Oka , Hiroshi Masutani , Junji Yodoi , Hajime Nakamura . 2009. Thioredoxin-Binding Protein-2 Deficiency Enhances Methionine-Choline Deficient Diet-Induced Hepatic Steatosis But Inhibits Steatohepatitis in Mice. *Antioxidants & Redox Signaling* **11**:10, 2573-2584. [Abstract] [Full Text HTML] [Full Text PDF] [Full Text PDF with Links]